



NAVAL POSTGRADUATE SCHOOL

MONTEREY, CALIFORNIA

THESIS

TETHERED SPACECRAFT SYSTEMS FOR ACTIVE DEBRIS REMOVAL

by

Jessica R. Shapiro

December 2018

Thesis Advisor:

Dr. Marcello Romano

Second Reader:

Dr. Gregory Byrne

Approved for public release. Distribution is unlimited

THIS PAGE INTENTIONALLY LEFT BLANK

REPORT DOCUMENTATION PAGE			Form Approved OMB No. 0704-0188	
Public reporting burden for this collection of information is estimated to average 1 hour per response, including the time for reviewing instruction, searching existing data sources, gathering and maintaining the data needed, and completing and reviewing the collection of information. Send comments regarding this burden estimate or any other aspect of this collection of information, including suggestions for reducing this burden to Washington headquarters Services, Directorate for Information Operations and Reports, 1215 Jefferson Davis Highway, Suite 1204, Arlington, VA 22202-4302, and to the Office of Management and Budget, Paperwork Reduction Project (0704-0188) Washington DC 20503.				
1. AGENCY USE ONLY (Leave Blank)		2. REPORT DATE December 2018	3. REPORT TYPE AND DATES COVERED Master's Thesis MM-DD-YYYY to MM-DD-YYYY	
4. TITLE AND SUBTITLE TETHERED SPACECRAFT SYSTEMS FOR ACTIVE DEBRIS REMOVAL			5. FUNDING NUMBERS	
6. AUTHOR(S) Jessica R. Shapiro				
7. PERFORMING ORGANIZATION NAME(S) AND ADDRESS(ES) Naval Postgraduate School Monterey, CA 93943			8. PERFORMING ORGANIZATION REPORT NUMBER	
9. SPONSORING / MONITORING AGENCY NAME(S) AND ADDRESS(ES) N/A			10. SPONSORING / MONITORING AGENCY REPORT NUMBER	
11. SUPPLEMENTARY NOTES The views expressed in this document are those of the author and do not reflect the official policy or position of the Department of Defense or the U.S. Government. IRB Protocol Number: N/A.				
12a. DISTRIBUTION / AVAILABILITY STATEMENT Approved for public release. Distribution is unlimited			12b. DISTRIBUTION CODE	
13. ABSTRACT (maximum 200 words) This study will explore momentum exchange tethered systems for applications of active debris removal The focus will be on exploring orbital transfer methods and investigate retrieval of debris and will not include rendezvous or tether composition characteristics. The developed guidance and control method will be integrated into a dynamic model. Past and current systems will be reviewed, including the Gemini-11 tether test, and Tethered Satellite System. This study will be conducted via computer simulation and analysis.				
14. SUBJECT TERMS			15. NUMBER OF PAGES 43	
			16. PRICE CODE	
17. SECURITY CLASSIFICATION OF REPORT Unclassified	18. SECURITY CLASSIFICATION OF THIS PAGE Unclassified	19. SECURITY CLASSIFICATION OF ABSTRACT Unclassified	20. LIMITATION OF ABSTRACT UU	

NSN 7540-01-280-5500

Standard Form 298 (Rev. 2-89)
Prescribed by ANSI Std. Z39-18

THIS PAGE INTENTIONALLY LEFT BLANK

Approved for public release. Distribution is unlimited

TETHERED SPACECRAFT SYSTEMS FOR ACTIVE DEBRIS REMOVAL

Jessica R. Shapiro
Lieutenant, United States Navy
B.S., Systems Engineering, United States Naval Academy, 2012

Submitted in partial fulfillment of the
requirements for the degree of

MASTER OF SCIENCE IN ASTRONAUTICAL ENGINEERING

from the

**NAVAL POSTGRADUATE SCHOOL
December 2018**

Approved by:

Dr. Marcello Romano
Thesis Advisor

Dr. Gregory Byrne
Second Reader

Dr. Garth Hobson
Chair, Department of Mechanical and Aerospace Engineering

THIS PAGE INTENTIONALLY LEFT BLANK

ABSTRACT

This study will explore momentum exchange tethered systems for applications of active debris removal. The focus will be on exploring orbital transfer methods and investigate retrieval of debris and will not include rendezvous or tether composition characteristics. The developed guidance and control method will be integrated into a dynamic model. Past and current systems will be reviewed, including the Gemini-11 tether test, and Tethered Satellite System. This study will be conducted via computer simulation and analysis.

THIS PAGE INTENTIONALLY LEFT BLANK

Table of Contents

1	Introduction	1
1.1	Orbital Debris	2
1.2	Tethered Spacecraft Systems	7
1.3	Research Objectives and Thesis Organization	8
2	Astrodynamics	11
2.1	Classical Orbital Elements.	11
2.2	Two-Body Problem	11
2.3	Coordinate Systems	12
2.4	Satellite Relative Motion	15
3	Orbital Debris Lifetime Analysis	17
3.1	Debris Characteristics	17
3.2	Debris Lifetime Analysis	17
	List of References	21
	Initial Distribution List	25

THIS PAGE INTENTIONALLY LEFT BLANK

List of Figures

Figure 2.1	Classical Orbital Elements [1]	12
Figure 2.2	Chief and Deputy Spacecraft Local Vertical-Local Horizontal with ECI frame	15
Figure 3.1	Effect of increasing drag area on orbital lifetime	18
Figure 3.2	Effect of increasing drag area on orbital lifetime - 50 km tether comparison	19
Figure 3.3	Effect of increasing tether length on orbital lifetime - 10 m sphere radius	20

THIS PAGE INTENTIONALLY LEFT BLANK

List of Tables

Table 1.1	Summary of Space Tether Missions	9
Table 3.1	Debris characteristics	18

THIS PAGE INTENTIONALLY LEFT BLANK

List of Acronyms and Abbreviations

DoD	Department of Defense
NPS	Naval Postgraduate School
USN	U.S. Navy
USG	United States government
TSS	Tethered Satellite System
ECI	Earth Centered Inertial
ECEF	Earth Centered-Earth Fixed
LVLH	Local Vertical Local Horizontal
RAAN	Right Ascension of the Ascending Node
DCM	Direction Cosine Matrix
ISAS	Institute of Space and Astronautical Sciences
EDT	Electro Dynamic Tether
CW	Clohessy-Whiltshire
STELA	Semi-analytic Tool for End of Life Analysis
ADR	Active Debris Removal
LEO	Low Earth Orbit
PMD	Post Mission Disposal
CNES	National Centre for Space Studies
HST	Hubble Space Telescope

ISS	International Space Station
ODPO	Orbital Debris Program Office
NASA	National Aeronautics and Space Administration
DARPA	Defense Advanced Research Projects Agency
IADC	Inter-Agency Space Debris Coordination Committee

Acknowledgments

Thanks!

THIS PAGE INTENTIONALLY LEFT BLANK

CHAPTER 1:

Introduction

One of the major issues facing future operations in space is the rapidly increasing population of orbital debris, or space junk in Earth's orbit. Orbital debris is comprised of defunct human-made objects over a wide range of sizes; objects larger than about 10 cm are trackable and cataloged in the U.S. Space Surveillance Catalog. Active Debris Removal (ADR) methods have been proposed and unless ADR is implemented, the space junk population will increase dramatically, presenting hazards to current and future space missions. Tethered methods of active debris removal present an intriguing solution that should be investigated and the benefits compared to other methods of active debris removal.

This study consists of surveys of tethered space systems and active debris removal methods with a focus on tethered space tugs and momentum-exchange systems. To maintain a reasonable scope for this project, the debris will be assumed to have been captured, with the tether attached to the center of mass of both the debris and the removal vehicle. The debris analyzed is an intact spacecraft with simplified characteristics loosely based on Hubble Space Telescope (HST).

This study will then compare the results of different removal methods, including the addition of a drag sail to the debris, the addition of a drag sail via a long tether, tethered momentum-exchange orbital transfers, and propulsive orbital transfers. The tethered-sail system model will offer a parametric comparison exploring how changes in tether length and orbital altitude differences affect deorbit time. It is assumed that the drag sail area remains constant and the drag sail system is attitude controlled to utilize the maximum drag area. The momentum-exchange model will explore effects of tether length on the momentum-exchange orbital transfer. The goal of this thesis is to show that tethered ADR solutions are feasible and can be more effective than other proposed ADR methods. This chapter begins by reviewing orbital debris mitigation practices, followed by the current state of active debris removal. As the goal for this thesis is to specifically investigate tethered ADR systems, section 1.2.1 also includes a survey of tethered space systems.

1.1 Orbital Debris

There are currently more than 20,000 known, monitored objects larger than 10 cm that present debris hazards in the Low Earth Orbit (LEO) environment (up to 2000 km). The debris includes non-operational spacecraft; derelict launch vehicle stages; mission-related debris such as sensor covers, engine covers, straps, etc., which were typically considered expendable parts in missions from the 60s and 70s; or fragmentation debris, which can be due to anomalous events, explosions, or collisions [2]. The debris population fluctuates as a function of solar flux (and thereby, atmospheric density) and of major debris generating events, such as the 2007 Fengyun-1C Chinese anti-satellite missile test and the 2009 Cosmos and Iridium collision.

Debris from events such as these increased the hazard to space assets and further endangers human spaceflight missions. For example, The International Space Station (ISS) is required to maneuver if there is a debris collision risk greater than 1 in 100,000 and mission objectives would not be compromised, requiring propellant usage. If the risk of collision is too great, and ISS is unable to maneuver, the crew must board the Soyuz spacecraft to prepare to undock [2]. These risks are currently manageable, but as the debris population increases, so will the risk to space assets. Additionally, as the amount of debris grows, shielding solutions will have to be implemented on future launches [2]. Moreover, satellite constellations are rapidly becoming a popular option for aerospace companies, but as these satellites become inoperable with age they will add to the orbital debris pollution problem in LEO. In order to protect the LEO environment, where we do most of our satellite business, a recent study on large constellations by National Aeronautics and Space Administration (NASA)'s Orbital Debris Program Office (ODPO) determined that 99 percent of satellites need to be de-orbited within five years upon conclusion of their mission. Large constellations will potentially add thousands of small satellites to an already congested environment, so even with a best-case scenario of 99 percent success rate of post-mission disposal of constellation satellites (in addition to post-mission disposal of normal LEO satellites), the implementation of large constellations would still add to the debris population by 22 percent over the next 200 years [3].

Models have shown that the debris population in LEO will continue to increase in a runaway nonlinear fashion, even if all future launches are stopped, due to collisions between orbiting objects, a phenomenon known as the Kessler Syndrome, identified by NASA in 1978 [4].

As the debris population increases, the risk of collision increases, and further collisions and explosions create new debris in an endless positive feedback loop. During a technical seminar in 2011, NASA's chief scientist for orbital debris, J.-C. Liou, reported that, as the debris population increases, more frequent conjunction assessments will be needed; more collision avoidance maneuvers will need to be made; more debris impact shields will be needed, which adds more mass requirements to future systems and limits launch capability; and the risk for potential critical failures due to collisions or explosions will increase [5]. Likewise, projections show that without post-mission disposal or other mitigation, over the next 200 years the number of debris objects in LEO experiences a 330 percent population increase with dramatic catastrophic collision potential [3].

A 2009 baseline study by NASA's ODPO study determined that even if all future launches were suspended, and even if post-mission disposal of re-entry within 25 years in accordance with debris mitigation policies was 90 percent successful, the debris population would still increase by 75 percent over the next 200 years. However, this same study determined that by implementing an ADR program, the debris population is in fact manageable; by removing at least five objects a year, the debris population can be held relatively constant. Currently, though, ADR is not a commonly practiced solution because it is technically difficult and expensive. Further complicating the issue is that international treaties prohibit the removal of space objects by anyone other than their owner, so there are political factors such as ownership and liability to consider.

1.1.1 Orbital Debris Mitigation

In an effort to limit future debris creation events, many policies have been implemented by the spacefaring nations. The Inter-Agency Space Debris Coordination Committee (IADC) is an international governmental forum for the worldwide coordination of activities related to the issues of man-made and natural debris in space. Current IADC Orbital Debris Mitigation Policy states that upon completion of its mission, a satellite shall either reenter the atmosphere within 25 years, or shall be removed to a storage orbit during a process called Post Mission Disposal (PMD). NASA refers to this policy as "design for demise" whereby all current launches must include some end-of-life disposal methods to adhere to this policy and reduce the risk of casualty [2]. Disposal methods include the use of drag enhancement devices, or including the propellant required for propulsive deorbit, or

transfer to a graveyard orbit in the propellant budget. Drag enhancement involves increasing the cross-sectional area of the system to exploit atmospheric drag to increase the rate of orbital decay. The method of adding a drag enhancement device to a tethered system will be investigated in chapter 4. For satellites without maneuvering capabilities, mission orbits are often simply chosen in which natural atmospheric drag will deorbit the object within 25 years. This straightforward approach is popular with many of the newer CubeSat experiments [6]. Additionally, passivation is required upon mission completion to prevent explosions of upper stages.

However, as discussed previously, PMD alone is insufficient to protect the space environment. Additional policy changes have been suggested to impose taxation to fund cleanup efforts and limit future launches. There is however, concern that this would limit the accessibility of space and is unfair to smaller space agencies as most of debris is from three major players (United States, Russia, and China) [2]. While PMD offers a solution to future debris remediation, ADR methods can be applied to persistent non-compliant debris that has been a high risk to further polluting the LEO environment for many years [6]. Due to the cost and complexities involved in ADR, the debris candidates for ADR must be prioritized and selected carefully. The removal criterion is determined by debris mass and its collision probability over time. Once an object has been selected for removal, it must be removed quickly to mitigate its collision risk [4].

1.1.2 Active Debris Removal Concepts

In a 2013 internal report, NASA identified several major strategies for ADR methods for large debris removal. In particular, they reviewed drag enhancement devices such as drag sails and inflatables, lasers, Electro Dynamic Tether (EDT) space tugs, the Geosynchronous Large Debris Deorbiter (GLiDeR) concept, Frozen mist, ballistic intercept, tungsten dust, laser collision avoidance, and the ion beam shepherd [7].

In September 2018, Surrey Satellite’s removeDebris payload demonstrated successful debris capture with its on-board net technology in the first successful demonstration of ADR technology in human history [8]. This payload contains additional experiments for vision-based navigation for non-cooperative rendezvous, a harpoon debris capture experiment with a 25 m tether, and a drag sail demonstration [9].

Other upcoming ADR missions include ESA's Clean Space initiative which is developing the e.deorbit satellite to remove a large piece of debris, and the CleanSat program which aims to develop technologies to ensure that future satellites are able to comply with debris regulations [10]. e.deorbit hopes to launch in 2023. Its mission is to capture a large piece of ESA-owned debris in the 800-1000 km altitude range, in a near polar orbit and is considering net capture, or robotic arms with grippers to capture its target [11]. The ultimate deorbit method considered resembles a space tug. Space tugs are debris removal vehicles that rendezvous and grapple a debris object to relocate it into a disposal orbit, usually via propulsive means.

CleanSpaceOne is a proposed ADR technology demonstration to capture Swiss-owned SwissCube [10]. Challenges for this demonstration include detection and capture, due to SwissCube's small size and high tumble rate. As of this year, this project is still in the funding consolidation phase [12].

The GLiDeR concept proposes using active charge emissions and directed charged particles to increase the absolute electric potential of a debris object and deposit it into a graveyard orbit. This method is unique in that debris objects can be moved into its disposal orbit without requiring any physical contact between the GLiDeR and the debris [13].

Lasers are also being investigated as a debris removal method. A laser could potentially vaporize a portion of the debris, generating a thrust which causes the debris to alter its orbit [2]. There is, however concern about this method's potential interference with operational satellite. Sweeper satellites could be used in conjunction with this method to remove small debris particles [6].

The NASA 2013 report concluded that drag enhancement devices, space tugs, and electrodynamic tethers were the most viable large debris removal concepts based on mission suitability, technology readiness, schedule, risks and cost. This drives the motivation of this study for investigation into these methods in particular [7]. A tethered ADR system would reduce the fuel requirement for a de-orbit system and can be completely passive. Tethered space tug systems are being considered due to the advantages of being light weight, flexible, and with simple controller design. Several companies are developing electrodynamic terminator tether tape technologies for smallsats and cubesats. A conductive tether induces an electric potential generated by its motion through the earth's magnetic field; the resultant

Lorentz force slowly deorbits the object [2]. Patents have been developed by Researchers at the Universidad Carlos III de Madrid for power generation via tethers as a satellite lowers in altitude, transforming orbital energy into electromagnetic energy via passive exploitation of Lorentz drag to remove inactive satellites [14].

Additionally, momentum tethers are an option considered by NASA [2]. Momentum tethers use the rotation of a debris removal vehicle to generate momentum and remove the object to a lower orbit once the tether is severed on the principle of dynamic release. This method in particular will be investigated thoroughly in chapter 5. A momentum tether scenario proposed by NASA involves attaching a non-conductive tether to a piece of orbital debris, generating momentum by swinging the tether back and forth with a mechanism, then severing the tether to use the generated momentum to swing the object out of orbit. This method may effectively deorbit large masses, which is the greatest concern for collision risks [2]. A momentum exchange tether system is also a solution worth investigation because these systems can also be used for propellantless formation flight and stationkeeping. The "TAMU sling sat sweeper" concept proposes using inelastic collisions to capture debris and using a change in angular rate to appropriately expel the debris with the desired conditions. Additionally, the momentum exchange from this maneuver can be used to assist in orbital transfer to a subsequent debris for capture, minimizing the necessary propellant used by the sweeper vehicle [15].

The most cost effective space tugs mission would be able to service multiple debris objects [6]. There are many technical challenges to this method. Rendezvousing with and grappling a tumbling debris object requires very sophisticated guidance and control, and the grappling mechanism must be robust enough to accommodate all sorts of extended structures and odd shapes [6]. The European company Airbus is also developing a space tug for on-orbit maintenance and debris removal. Airbus developed the debris capture net that was demonstrated on the removeDebris mission, as well as the harpoon capture system, and the visual based navigation system that will be demonstrated in the following stages of the mission [8].

In 2017 Defense Advanced Research Projects Agency (DARPA) awarded Space Systems Loral (SSL) the contract for their Robotic Servicing of Geosynchronous Satellites (RSGS) program, which includes relocation and other orbital maneuvers. This program will also

develop many of the technologies and techniques that can be applied to ADR. SSL's RSGS payload is anticipated to launch in 2021 [16].

1.2 Tethered Spacecraft Systems

Tethered ADR methods are some of the primary researched methods by major space industry players because the advantages of implementing tethers in space have been apparent since before the dawn of the space program. Many applications of tethered space systems have been studied and explored, including propellantless formation flying, momentum exchange maneuvers, debris removal and towing, aerobraking for deorbiting maneuvers, power generation or propulsion via electrodynamic tethers, generating microgravity for on-orbit refueling, and, upper atmosphere exploration [17].

1.2.1 Review of Tethered Space Missions

The first concept of a tethered space system was developed in 1895 by Russian scientist Konstantin Tsiolkovsky when he conceived the idea for a "space elevator." [18]. This was followed by Yuri Artsutanov's concept in 1960 when he published the idea of using a geostationary satellite as a base to deploy a structure toward earth using a counterweight to maintain a stationary center of gravity [19]. In 1966, Gemini-11 conducted a 30 m tethered experiment to generate .0005g of artificial gravity via the spin between the capsule and the target vehicle [20]. The following mission Gemini-12 demonstrated tethered station-keeping with the Agena target vehicle and gravity-gradient vertical stability [21].

The early 1980s produced several joint experiments between NASA and Institute of Space and Astronautical Sciences (ISAS). TPE-1, TPE-2, Charge-1, Charge-2, were all suborbital sounding rocket tests with electrodynamic tethers to study upper atmospheric conditions. Charge-2 utilized control thrusters to maintain tether tension. OEDIPUS-A and C were sounding rocket experiments with NASA and Canada to provide data about the ionosphere [21].

TSS-1 was a joint NASA/Italian Space Agency (ISA) mission launched in 1992 on STS-46 and deployed 268m above the orbiter, demonstrating the feasibility of a gravity gradient stabilized system [22], TSS-1R was the follow-on mission flown on STS-75 in 1996. The goal was a 20.7 km tether deployed from the Space Shuttle Columbia for space

plasma physics experiments [23]. The tether managed to deploy to 19.6 km, but severed due to electric arcing within the tether, inadvertently demonstrating momentum exchange on both the shuttle and the deployed satellite as both were moved into new, elliptical orbits [21]. The Small Expendable Deployer System Missions (SEDS) used active braking and feedback control for tether deployment and to limit residual swing and proved several stability concepts [21]. The Plasma Motor Generator (PMG) in 1996 was a conducting tether that proved that orbital energy could be converted into electrical energy and the ability to use electrostatic tethers as an orbit boosting device, vice propellant. [19]. Tether Physics and Survivability Spacecraft (TiPS) employed a larger diameter tether to ensure resilience to severing and studied long term tether dynamics and remained in orbit for over 10 years. [24]. Most of the failures for these missions are due to deployment problems, or tether severing due to manufacturing faults, parent satellite safety considerations, or cut due to impact. A summary of tethered missions is provided in Table 1.1.

1.2.2 Tethered Spacecraft Dynamics

In this thesis, the tethered debris removal system will be modeled as a dumbbell spacecraft system. The dumbbell spacecraft system consists of two satellites connected by a rigid, massless tether. This system can be described as a rigid body, exhibiting a pendular motion about the system's center of mass. Coupling effects are studied by using the radial motion, orbital motion, and in-plane libration motion [25]. Libration refers to the perceived oscillation of orbiting bodies relative to each other *i.e.*, the oscillating motion about a point of equilibrium [26]. The dynamics of this system will be explored in depth in later chapters.

1.3 Research Objectives and Thesis Organization

The goal of this thesis is to develop a comparison of two tethered methods of ADR: a space tug with the addition of a drag device, and a momentum exchange tethered system. This will be done via parametric analyses and observation of the dynamical model of each method. These methods will be compared to an optimized propulsive deorbit method.

The remainder of this thesis is divided into 7 chapters. Chapter 2 provides a review of applicable astrodynamics concepts, chapter 3 will offer a baseline analysis on the orbital lifetime of the debris object candidate for ADR, chapter 4 will present an analysis on a

Table 1.1. Summary of Space Tether Missions

Name	Year	Orbit	Length	Agency	Comments
Gemini-11	1966	LEO	30 m	NASA	Spin stable 0.15 rpm
Gemini-12	1966	LEO	30 m	NASA	Local vertical, stable swing
TPE-1	1980	Suborbital	500 m	NASA/ISAS	EDT Partially deployed 38m
TPE-2	1981	Suborbital	500m	NASA/ISAS	Partially deployed 65 m
Charge-1	1983	Suborbital	418m	NASA/ISAS	Fully deployed
Charge-2	1984	Suborbital	426m	NASA/ISAS	Fully deployed
Oedipus-A	1989	Suborbital	958m	CSA/NASA	Spin stable @ 7 Hz, magnetic field aligned
Charge-2B	1992	Suborbital	500m	NASA	Fully deployed
TSS-1	1992	LEO	260m	NASA/ISA	Partially deployed, retrieved
SEDS-1	1993	LEO	20 km	NASA	Downward fully deployed, swing, and cut
PMG	1993	LEO	500m	NASA	Upward deployed
SEDS-2	1994	LEO	20km	NASA	Fully deployed, local vertical, stable
Oedipus-C	1995	Suborbital	1170 m	CSA/NASA	Spin stable @ 5 rpm, magnetic field aligned
TSS-1R	1996	LEO	19.6 km	NASA/ISA	Close to full deployment, severed by arcing
TiPS	1996	LEO	4 km	NRO/NRL	Long-life tether on-orbit (survived 12 years)
ATEX	1999	LEO	6 km	NRL	Partially deployed (22 m)
ProSEDS	1999	LEO	15 km	NASA	Hardware build but not flown
DTUsat-1	2003	LEO	450 m	TUD	Nano-Satellite failed to work in space
MAST	2007	LEO	1 km	NASA	Tether failed to deploy
YES2	2007	LEO	30 km	ESA	Fully deployed
Cute-1.7+APDII	2008	LEO	10 m	Tokyo Tech, Japan	Cube-Satellite worked, Tether failed to deploy
STARS	2009	LEO	10 km	Kagawa U, Japan	Space tethered robot mission, tether not fully deployed
T-Rex	2010	Suborbital	300 m	JAXA	Tether deployed, current not measured
STARS-II	2014	LEO	300 m	JAXA	Electrodynamic tether deployment not confirmed
KITE	2016	LEO	700 m	JAXA	Deployment failure
STARS-C	2016	LEO	100 m	JAXA	Tether deployment not confirmed
removeDebris	2018	LEO	25 m	ESA	Harpoon debris capture demo

space tug with a drag enhancement device implementation, chapter 5 explores momentum exchange ADR methods, and chapter 6 will explore optimization for propulsive deorbit. Finally, chapter 7 offers a summary, conclusions, and recommendations for areas of future research into tethered ADR.

CHAPTER 2: Astrodynamics

To evaluate the viability of tethered ADR, it will be necessary to draw upon a number of concepts in the field of orbital mechanics. This section provides an overview of several of these concepts and offers a preliminary analysis of their applicability to tethered ADR.

2.1 Classical Orbital Elements

The Classical Orbital Elements, shown in Figure 2.1 are the parameters by which the orbit of any spacecraft, such as an ADR system, is described, shown in the structure below [26].

$$\alpha = \{a, e, i, \Omega, \omega, \nu\}$$

a is the semi-major axis of the elliptical orbital plane and describes the size of the orbit. The eccentricity, e , describes the shape of the orbit and $0 \leq e < 1$ for all closed orbits. In vector form, the eccentricity vector points from apogee to perigee. i is the inclination, or the angle from the equatorial plane to the orbital plane. The right ascension of the ascending node, Ω , refers to the angle from the geocentric axis pointing to the first point of Aries, shown in figure 2.1 as the X axis, to the node line, which is the intersection of the orbital plane and the equatorial plane [1]. The ascending node is referred to as such because it is the point on the orbit where the object moves north through the plane [27]. ω is the argument of perigee and refers to the angle between the line pointing to the ascending node and the perigee direction of the satellite motion. In this thesis, as all orbits described are Earth orbits, the terms periapsis and perigee may be used interchangeably. The true anomaly ν describes the position of the object along its orbital path described as the angle between the direction of periapsis and the current position. The inertial position and velocity of a spacecraft depend on time and the classical orbital elements.

2.2 Two-Body Problem

To accurately describe the dynamics of a tethered ADR system, the motion of the system as a whole must be considered in its orbit around Earth. This is given by the classical

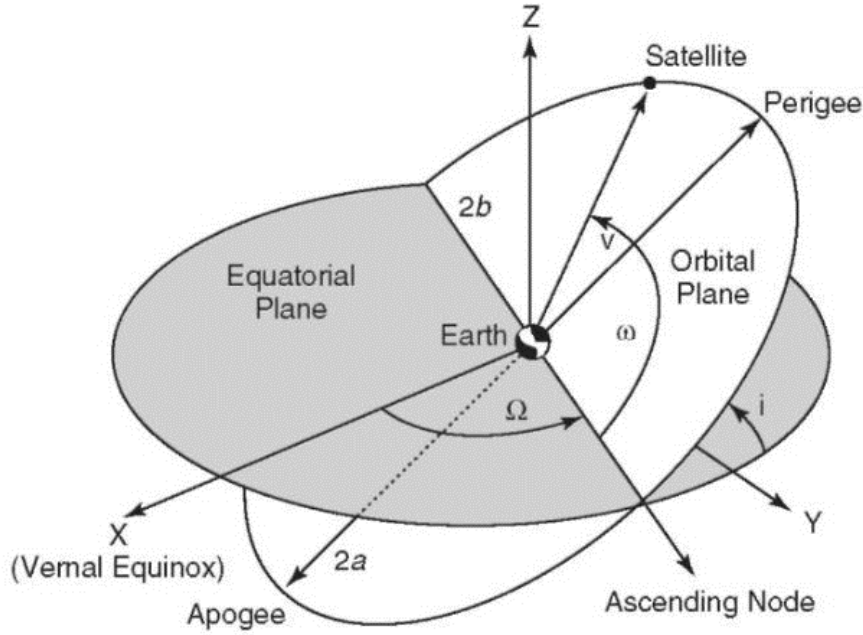


Figure 2.1. Classical Orbital Elements [1]

Keplerian two-body problem. The two-body problem states:

$$\ddot{\mathbf{r}} = \frac{-\mu}{r^3} \mathbf{r} \quad (2.1)$$

for any satellite position \mathbf{r} , where μ is the standard gravitational parameter used in celestial mechanics, and $\mathbf{r} = [X, Y, Z]^T$, the satellite's position vector in the Earth Centered Inertial (ECI) frame. The gravitational parameter is equal to the product of Newton's gravitational constant, G , and the mass of the Earth [27], given by

$$\mu = 3.98 * 10^5 \frac{km^3}{s^2}$$

Using the orbital elements to determine the positional and velocity components of the system's orbit, the Keplerian equations of motion can be numerically solved to determine the motion of the system as a function of time. This depiction of the two-body equation of motion assumes a spherical earth and neglects tidal forces [26].

2.3 Coordinate Systems

To accurately describe the kinematics of a tethered system, reference frames must be established to describe different coordinate systems. In this section, the applicable fixed

and rotating reference frames are defined.

2.3.1 Earth Centered Inertial - ECI

The ECI frame is a *geocentric* Cartesian coordinate system with its origin at the center of the Earth with the unit vector $\hat{\mathbf{X}}$ towards the Vernal Equinox, the unit vector $\hat{\mathbf{Z}}$ normal to the fundamental plane of the equator, and the unit vector $\hat{\mathbf{Y}}$ completing the set, as seen in figures 2.1 and 2.2. This reference frame remains fixed while the Earth rotates.

2.3.2 Perifocal

The perifocal coordinate system is a fixed reference frame centered at the focus of the orbit, in this case Earth, with the orbital plane as the fundamental plane. This system is considered the "natural frame" for an orbit [27]. The $\hat{\mathbf{x}}$ vector is in the plane in the direction of the periapsis, *i.e.*, along the eccentricity vector, and the $\hat{\mathbf{y}}$ vector is rotated 90° in the plane in the direction of orbital motion. The $\hat{\mathbf{z}}$ vector is normal to the orbital plane in the direction of the orbital angular momentum vector \mathbf{h} . These unit vectors are also often described with the notation \mathbf{p} , \mathbf{q} , and \mathbf{w} , for \mathbf{x} , \mathbf{y} , and \mathbf{z} , respectively [28].

Coordinate Transformation

Inertial differential equations are typically expressed in the perifocal frame but to understand the inertial position represented here, a rotation matrix is required to transfer the coordinates into the ECI frame. The transformation from the Perifocal Frame to the ECI frame can be accomplished with a 3-1-3 rotation sequence as follows:

1. Rotate the frame by ω about the angular momentum vector \mathbf{h}
2. Rotate by the frame by i about the vector in the direction of the ascending node \mathbf{I}
3. Rotate by the frame by Ω about the ECI's \mathbf{z} unit vector

The composite rotation from the Perifocal to the ECI frame is

$$\mathbf{r}_{ECI} = R_3(\Omega)R_1(i)R_3(\omega)$$

Which gives the Direction Cosine Matrix (DCM)

$$\mathbf{C} = \begin{bmatrix} \cos \Omega \cos \omega - \sin \Omega \sin \omega \cos i & -\cos \Omega \sin \omega - \sin \Omega \cos \omega \cos i & \sin \Omega \sin i \\ \sin \Omega \sin \omega + \cos \Omega \sin \omega \cos i & -\sin \Omega \sin \omega + \cos \Omega \cos \omega \cos i & -\cos \Omega \sin i \\ \sin \omega \sin i & \cos \omega \sin i & \cos i \end{bmatrix}$$

[26]

2.3.3 Local Vertical Local Horizontal - LVLH

The Local Vertical Local Horizontal (LVLH) coordinate system is a *rotating* frame centered at the spacecraft. The fundamental plane is the orbital plane of the satellite, with the $\hat{\mathbf{z}}$ normal to the plane, pointing in the direction of the orbital momentum vector \mathbf{h} . The $\hat{\mathbf{x}}$ vector is in the plane, pointing radially outward from the spacecraft, as seen in figure 2.2. The $\hat{\mathbf{y}}$ completes the set and points in along-track direction of instantaneous velocity. This frame is also as Hill's frame [26]. In terms of formation flight, a deputy spacecraft is often described in terms of the chief's LVLH coordinates. This can be seen in Figure 2.2 where the \mathbf{R} vector points to the chief satellite, and sets the origin by which the deputy position \mathbf{r} is established. The LVLH unit vectors are derived from the position and velocity vectors in the ECI frame as follows [29]:

$$\begin{aligned} \hat{\mathbf{x}} &= \frac{\mathbf{r}_0}{|\mathbf{r}_0|} \\ \hat{\mathbf{z}} &= \frac{\mathbf{h}}{|\mathbf{h}|}, \quad \text{where} \quad \mathbf{h} = \mathbf{r}_0 \times \mathbf{v}_0 \\ \hat{\mathbf{y}} &= \hat{\mathbf{z}} \times \hat{\mathbf{x}} \end{aligned}$$

The DCM to convert from ECI vectors to LVLH vectors is

$$[ON] = \begin{bmatrix} \hat{\mathbf{x}}^T \\ \hat{\mathbf{y}}^T \\ \hat{\mathbf{z}}^T \end{bmatrix}$$

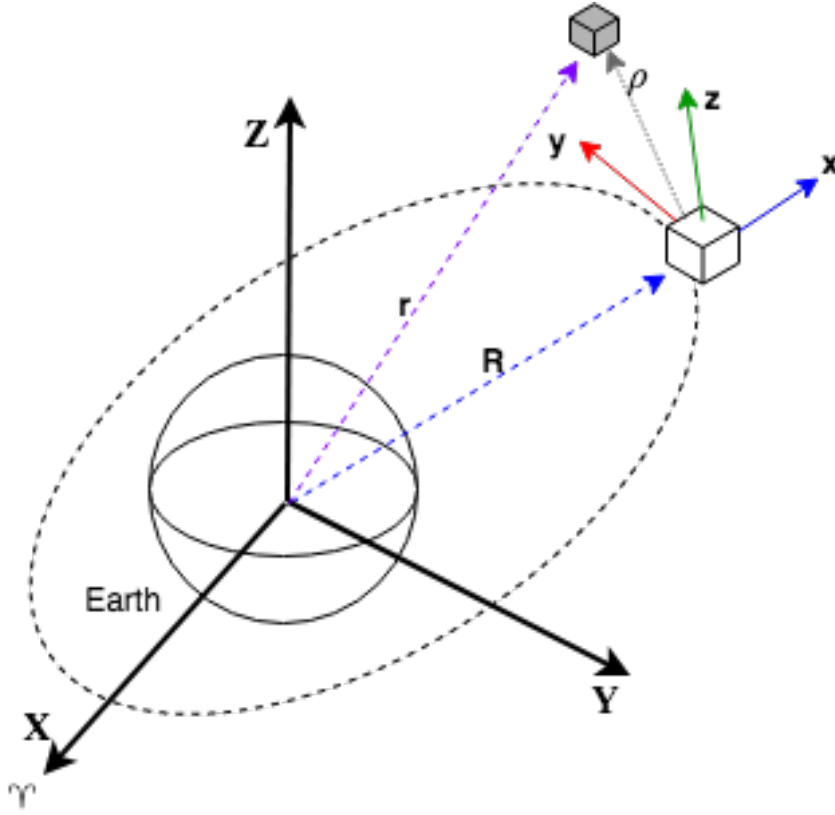


Figure 2.2. Chief and Deputy Spacecraft Local Vertical-Local Horizontal with ECI frame

2.4 Satellite Relative Motion

Relative motion is the depiction of the movement of a satellite with respect to another satellite. For convention, the debris removal satellite that will be used for reference will be referred to throughout as the *chief*, and the object, or uncontrolled debris, whose motion is described in terms of the chief will be referred to as the *deputy*. The position of the chief satellite is denoted by the vector \mathbf{R} and the position of the deputy is denoted by the vector \mathbf{r} . The vector describing the distance between the two satellites is denoted by the vector ρ shown in figure 2.2 The chief position vector in the LVLH frame is described by the following equation

$$\mathbf{R} = R\mathbf{i} \quad (2.2)$$

and the deputy relative motion vector can be described as

$$\mathbf{r} = \mathbf{R} + \boldsymbol{\rho} \quad (2.3)$$

Appendix A.1 contains an exploration of different methods of propagating relative motion using the Clohessy-Whiltshire and Tschauner-Hempel equations [26]. The Clohessy-Whiltshire method provides a simplified technique to solve the relative motion propagation of a circular orbit, but the Tschauner-Hempel equations can provide a more general simplified solution for any orbit using what is known as the Yamanaka-Ankersen method [34].

CHAPTER 3:

Orbital Debris Lifetime Analysis

In order to assess how ADR methods can impact a debris object, a baseline lifetime analysis was conducted on the candidate debris. The lifetime is determined as a function of orbital characteristics, spacecraft drag area, and atmospheric drag. The National Centre for Space Studies (CNES) developed software Semi-analytic Tool for End of Life Analysis (STELA) was used to conduct the lifetime analysis.

3.1 Debris Characteristics

The debris modeled throughout this study has the characteristics presented in Table 3.1 based loosely on those of Hubble Space Telescope. [30] For the purpose of maintaining a simple model, the debris will be modeled as a sphere, as will any debris removal vehicle. As the orbit represented here is circular, the terms altitude and semi-major axis are used interchangeably.

Additionally, it is assumed that despite the relatively short predicted lifetime of the debris, uncontrolled reentry is not an option due to the associated risks. A reentry survivability assessment of Hubble performed in 2005 predicts a reentry risk of 1:250, which well exceeds the acceptable risk of 1:10,000 [31] [32]

3.2 Debris Lifetime Analysis

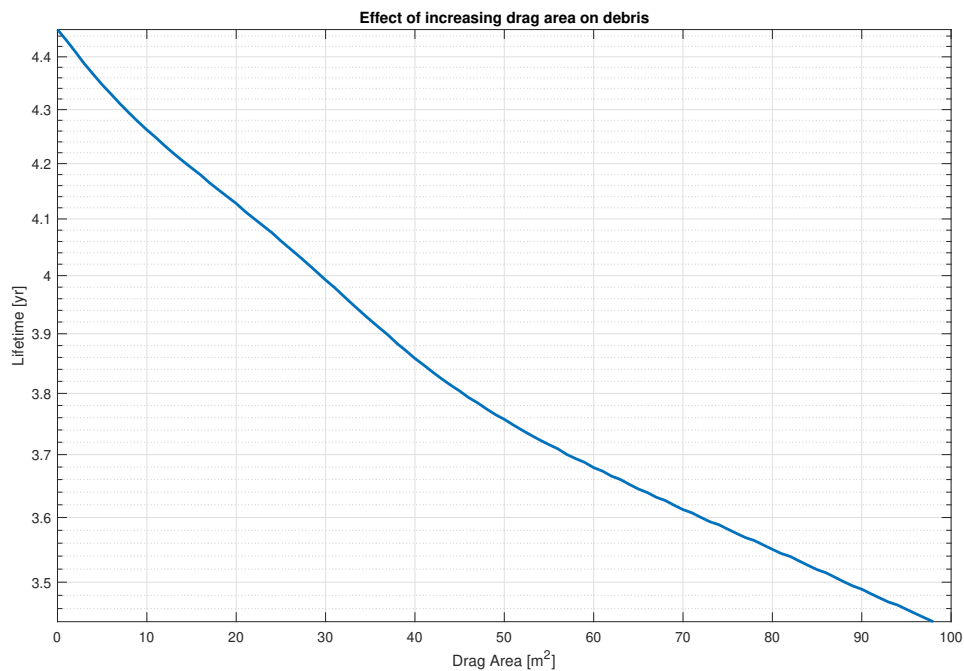
To determine the effect of increasing drag area on the debris, STELA was used to iteratively increase the drag area and determine the impact on orbital lifetime. Without drag area augmentation, the debris will reenter the atmosphere approximately 4.45 years from the start date epoch. While this is in compliance with DoDI 3100.12 section 6.4.1, the accepted practice of decaying within 25 years upon completion of missions, it is assumed that an uncontrolled entry is not an acceptable option due to reentry casualty risk. When an additional 100 m² are added to the debris, the debris decays in 3.44 years, as shown in figure 3.1. This suggests that this debris object is relatively insensitive to drag area augmentation

Table 3.1. Debris characteristics

Mass	10,000 kg
Sphere radius	5 m
Mean drag area	78.6 m ²
Epoch	August 15, 2018 21:40:27 UTC
Inclination	28.5°
Semi-major axis	6878 km
Eccentricity	0
Right Ascension of the Ascending Node (RAAN)	80°
Argument of perigee	65°
Mean Anomaly	24°

alone. The atmospheric model used to model atmospheric drag was NRLMSISE-00 and the solar activity was variable beginning from the epoch listed in table 3.1.

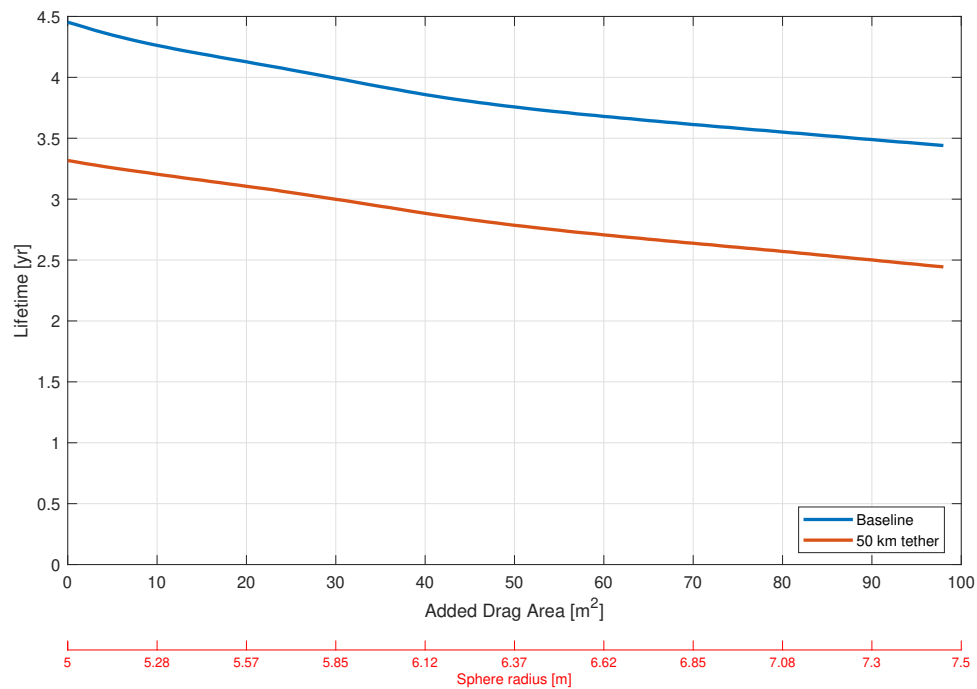
Figure 3.1. Effect of increasing drag area on orbital lifetime



The data presented in Figure 3.2 shows the same analysis as the previous, but the starting

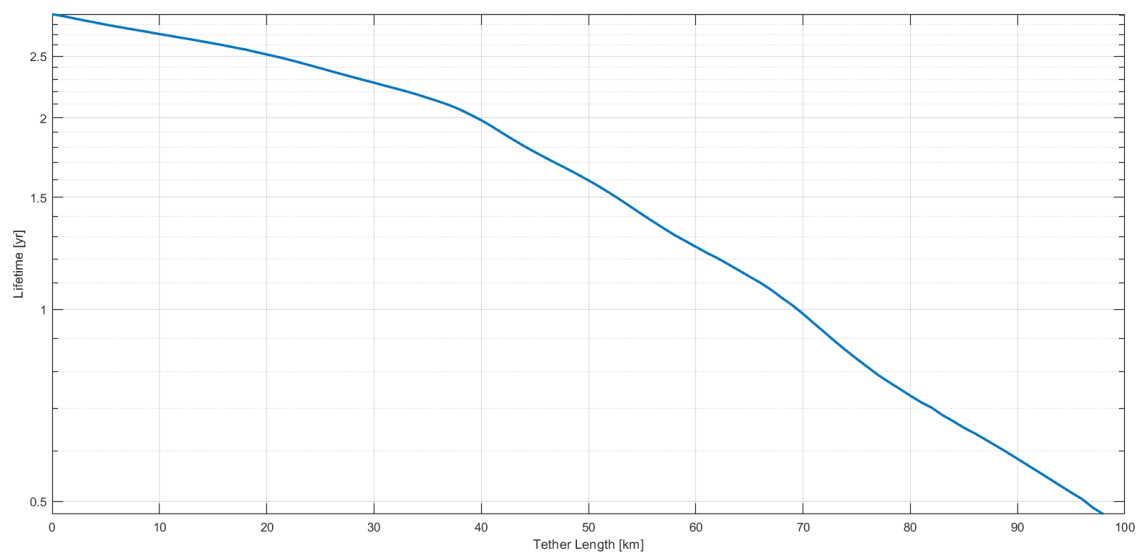
altitude was set 50 km lower than the baseline to represent a 50 km drag tether, represented as the red line. This data shows that with an additional 100 m^2 , the orbital lifetime can be reduced to 2.44 years. These lines display a near parallel trend, and the average difference in lifetime as area increases is about one year. The red axis below the axis displaying total drag area increase shows the total spherical radius of the object given by the increased drag area.

Figure 3.2. Effect of increasing drag area on orbital lifetime - 50 km tether comparison



To observe the effect of tether length over lifetime, a spherical object with a fixed radius of 10 m was assessed. The mass remained constant at 10,000 kg. To simulate increasing tether length, the starting altitude of the object's orbit was iteratively decreased, and the lifetime for each discrete iteration was determined. The data presented in figure 3.3 suggests that with a 70 km tether, a spherical object with a 10 m radius could reenter Earth's atmosphere within a year.

Figure 3.3. Effect of increasing tether length on orbital lifetime - 10 m sphere radius



List of References

- [1] G. Byrne, “Lecture notes in space technology and applications,” Naval Postgraduate School, 2018.
- [2] *Orbital debris management & risk mitigation*. NASA Academy of Program/Project and Engineering Leadership, 2012.
- [3] J.-C. Liou, M. Matney, A. Vavrin, A. Manis, and D. Gates, “NASA ODPO’s large constellation study,” *Orbital Debris News Quarterly*, vol. 22, no. 3, 2018.
- [4] J.-C. Liou, N. L. Johnson, and N. M. Hill, “Controlling the growth of future LEO debris populations with active debris removal,” *Acta Astronautica*, vol. 66, no. 5-6, pp. 648–653, mar 2010.
- [5] J.-C. Liou, “Orbital debris and future environment remediation,” in *OCT Technical Seminar*, 2011.
- [6] M. Sorge and G. Peterson, “How to clean space: disposal and active debris removal,” *Crosslinks*, Fall 2015.
- [7] G. Byrne, “NASA orbital debris environment remediation strategies,” Personal Communication, Oct. 2018.
- [8] Net successfully snares space debris. [Online]. Available: <https://www.surrey.ac.uk/news/net-successfully-snares-space-debris>
- [9] Earth observation portal. [Online]. Available: <https://directory.eoportal.org/web/eoportal/satellite-missions/r/removedebris>
- [10] B. Chaudhary, “Unconventional methods for space debris removal,” in *Space Safety is No Accident*, T. Sgobba and I. Rongier, Eds. Cham: Springer International Publishing, 2015, pp. 49–58.
- [11] E.deorbit: it is time to make active debris removal a reality for the european space sector. (2017, Jan.). ESA. [Online]. Available: <http://blogs.esa.int/cleanspace/2017/01/30/e-deorbit-it-is-time-to-make-active-debris-removal-a-reality-for-the-european-space-sector/>
- [12] Cleanspace one. (2016). EPFL Space Center. [Online]. Available: https://espace.epfl.ch/CleanSpaceOne_1

- [13] H. Schaub and D. F. Moorer, "Geosynchronous large debris reorbiter: challenges and prospects," *The Journal of the Astronautical Sciences*, vol. 59, no. 1-2, pp. 161–176, jun 2012.
- [14] J. R. Sanmartín, A. Sánchez-Torres, S. B. Khan, G. Sánchez-Arriaga, and M. Charro, "Optimum sizing of bare-tape tethers for de-orbiting satellites at end of mission," *Advances in Space Research*, vol. 56, no. 7, pp. 1485–1492, oct 2015.
- [15] J. Missel and D. Mortari, "Sling satellite for debris removal with Aggie sweeper." AAS/AIAA, Feb. 2011.
- [16] Robotic Payload for RSGS Mission Moves to Next Phase of Development. [Online]. Available: <https://www.darpa.mil/news-events/2018-08-17>
- [17] V. V. Beletsky and E. M. Levin, *Dynamics of space tether systems* (Advances in the Astronautical Sciences). American Astronautical Society, 1993, vol. 83.
- [18] K. D. Kumar, "Review of dynamics and control of nonelectrodynamic tethered satellite systems," *Journal of Spacecraft and Robotics*, 2006.
- [19] Y. Chen, R. Huang, X. Ren, L. He, and Y. He, "History of the tether concept and tether missions: A review," *ISRN Astronomy and Astrophysics*, vol. 2013, pp. 1–7, 2013.
- [20] NASA Space Science Data Coordinated Archive. Gemini-11. NSSDCA/COSPAR ID: 1966-081A. [Online]. Available: <https://nssdc.gsfc.nasa.gov/nmc/masterCatalog.do?sc=1966-081A>. Accessed Aug. 16 2018.
- [21] M. V. Pelt, *Space tethers and space elevators*. Berlin, Germany: Springer, 2009.
- [22] M. Dobrowolny and N. H. Stone, "A technical overview of TSS-1: the first tethered-satellite system mission," *Il Nuovo Cimento C*, vol. 17, no. 1, pp. 1–12, jan 1994.
- [23] D. C. Thompson, C. Bonifazi, B. E. Gilchrist, S. D. Williams, W. J. Raitt, J.-P. Lebreton, W. J. Burke, N. H. Stone, and K. H. Wright, "The current-voltage characteristics of a large probe in low earth orbit: TSS-1r results," *Geophysical Research Letters*, vol. 25, no. 4, pp. 413–416, feb 1998.
- [24] M. Cosmo and E. Lorenzini, "Tethers in space handbook," 01 1997.
- [25] A. Frias, "Modeling and control of spacecraft systems with couple orbital and attitude dynamics," Master's thesis, Ryerson University, 2010.
- [26] K. T. Alfriend, S. R. Vadali, P. Gurfil, J. P. How, and L. S. Breger, *Spacecraft Formation Flying*. Butterworth-Heinemann, 2010.

- [27] H. D. Curtis, *Orbital mechanics for engineering students*, 3rd ed. United Kingdom: Butterworth-Heinemann, 2014.
- [28] R. R. Bates, D. D. Mueller, and J. E. White, *Fundamentals of astrodynamics*. New York, NY: Dover Publications, Inc., 1971.
- [29] H. Schaub and J. L. Junkins, *Analytical mechanics of space systems*, J. A. Schetz, Ed. American Institute of Aeronautics and Astronautics, 2003.
- [30] ESA, “Hubble Space Telescope fact sheet,” accessed: 2018-10-01. Available: https://www.spacetelescope.org/about/general/fact_sheet/
- [31] R. Smith, K. Bledsoe, J. Dobarco-Otero, W. Rochelle, N. Johnson, A. Pergosky, and M. Weiss, “Reentry survivability analysis of the Hubble Space Telescope (HST),” in *Proceedings of the 4th European Conference on Space Debris*, 2005.
- [32] Department of Defense, “Space support instruction (DoD Instruction 3100.12),” Sep. 2000.
- [33] Z. Dang, “Solutions of Tschauner-Hempel equations,” *Journal of Guidance, Control, and Dynamics*, vol. 40, no. 11, pp. 2956–2960, nov 2017.
- [34] K. Yamanaka and F. Ankersen, “New state transition matrix for relative motion on an arbitrary elliptical orbit,” *Journal of guidance, control, and dynamics*, 2002.

THIS PAGE INTENTIONALLY LEFT BLANK

Initial Distribution List

1. Defense Technical Information Center
Ft. Belvoir, Virginia
2. Dudley Knox Library
Naval Postgraduate School
Monterey, California